A b i n i t i o calculations of dissociative electronic states of ClCN: Implications to the photodissociation dynamics of the cyanogen halides

Y. Y. Bai, G. A. Segal, and H. Reisler

Citation: The Journal of Chemical Physics **94**, 331 (1991); doi: 10.1063/1.460347
View online: http://dx.doi.org/10.1063/1.460347
View Table of Contents: http://scitation.aip.org/content/aip/journal/jcp/94/1?ver=pdfcov
Published by the AIP Publishing

Ab initio calculations of dissociative electronic states of ClCN: Implications to the photodissociation dynamics of the cyanogen halides

Y. Y. Bai,[a] G. A. Segal, and H. Reisler[b]
Department of Chemistry, University of Southern California, Los Angeles, California 90080-0482

(Received 20 July 1990; accepted 6 September 1990)

Ab initio configuration interaction calculations with full geometric optimization along the Cl–CN dissociation coordinate have been carried out for several electronic states of ClCN. The calculations treat all low-lying singlet and triplet states and yield the vertical transition probabilities and oscillator strengths, as well as angular dependences near the Franck–Condon (FC) region and least energy paths for several electronic states as a function of r_{CCl}. We find that the low-lying excited states derive from three electronic configurations: $\pi^3\sigma^*$, $\pi^3\pi^*$, and $\sigma\pi^4\sigma^*$. The lowest excited triplet and singlet states derive from the $\pi^3\sigma^*$ configuration and give rise to bent $^{1,3}A'$ and $^{1,3}A''$ states. States arising from the $\pi^3\pi^*$ configuration are linear (Σ and Δ states). There is evidence of surface crossings along the reaction coordinate between triplet states arising from the $\pi^3\pi^*$ configuration and those arising from the $\pi^3\sigma^*$ and $\sigma\pi^4\sigma^*$ configurations. These crossings can be induced by slight bending of ClCN causing lowering of the symmetry. The calculated vertical excitation energies are in good agreement with features of the absorption spectrum, and suggest that the A continuum of ClCN involves transitions to the $2\,^1A'$ and $1\,^1A''$ states. The implications to the photodissociation dynamics of the cyanogen halides are discussed.

I. INTRODUCTION

The photodissociation of the cyanogen halides (XCN; X = Cl,Br,I) has attracted considerable attention in the past 20 years.[1–30] Following the pioneering work of Wilson[2] and Simons[3,4] and their co-workers on the photodissociation of ICN leading to $CN(X\,^2\Sigma^+)$ and $CN(B\,^2\Sigma^+)$, respectively, more recent work has concentrated primarily on dissociation in the lowest absorption feature of the cyanogen halides known as the A continuum, leading asymptotically to two main dissociation channels:

$$XCN \rightarrow CN(X\,^2\Sigma^+) + X(^2P_{3/2}) \quad (1)$$

$$\rightarrow CN(X\,^2\Sigma^+) + X(^2P_{1/2}). \quad (2)$$

Both scalar and vector properties have been exploited in attempts to elucidate the photodissociation dynamics,[1–12,21–30] and fs time-resolved studies are proving to be useful probes of the dynamics as well.[13] The most complete set of results concerns the photodissociation of ICN,[1–20] and the results suggest a complicated picture, apparently involving several potential energy surfaces (PESs) and multiple surface crossings.[6,8–12,14]

With the aid of *ab initio* calculations of the relevant PESs, the photodissociation dynamics of triatomic molecules can be understood today in great detail.[31] However, the cyanogen halides present a particularly challenging case. As a result of the large spin–orbit interaction in the halogen atom, the A continuum is thought to involve transitions also to triplet states, at least for BrCN and ICN.[4] The dissociation dynamics is further complicated by the possibility of avoided crossings, conical intersections, and nonadiabatic couplings that may occur during fragment separation. Theoretical treatments of the dissociation dynamics have been severely limited by the absence of *ab initio* calculations that identify the order and nature of the excited states and the couplings between them. Model surfaces have been constructed that reproduce some experimental findings,[8,14,19,27,28] but the results, which are often model dependent, may not be unique and thus do not provide definitive proof in favor of a particular dissociation mechanism.

The ground state configuration of linear XCN is [4,32]

$$(1\sigma)^2(2\sigma)^2(3\sigma)^2(1\pi)^4(4\sigma)^2(2\pi)^4;\quad ^1\Sigma^+.$$

The molecules have 16 valence electrons, and therefore are linear in their ground electronic state. The lowest energy excited state configuration is unknown, but derives most likely either from the $\pi^3\sigma^*$ or $\pi^3\pi^*$ electronic configurations. The former is suggested in analogy with the halogens and CH_3I, whose lowest excited states all derive from the $\pi^3\sigma^*$ configuration. King and Richardson,[33] and later Felps *et al.*[34] assigned the lowest excited state(s) of the cyanogen halides to this configuration. The latter configuration is suggested in analogy with other 16 electron triatomic molecules (e.g., CO_2, and OCS), and the similarities between their photoelectron spectra and those of the cyanogen halides.[32] Rabalais *et al.*[32] and Simons and co-workers[4] adopted this configuration for the lowest excited states of the cyanogen halides. There is no real theoretical preference for one configuration over the other. For linear molecules, the $\pi^3\pi^*$ configuration leads, in the case of small spin–orbit coupling, to linear $^{1,3}\Sigma^+$, $^{1,3}\Sigma^-$, and $^{1,3}\Delta$ states (16 components), and the $\pi^3\sigma^*$ configuration leads to $^{1,3}\Pi$ states (total of 8 components).[35] For bent upper states, the Σ^+, and Σ^- states will transform into A' and A'' states, respectively, while the Π and Δ states will each evolve into a pair of A' and A''

[a] Present address: Bellaire Research Center, Shell Development Company, Houston, Texas 77025.
[b] Author to whom correspondence should be addressed.

states.[35(b)] The photoelectron spectra of the cyanogen halides indicate the existence of a σ nonbonding orbital centered on the N atom and close in energy to the π orbitals.[36] The promotion of an electron from this orbital can lead to $\sigma\pi^4\pi^*$ and $\sigma\pi^4\sigma^*$ manifolds of states. Asymptotically, six surfaces will correlate with ground state products.

In view of the central role that the cyanogen halides play in studies of photodissociation dynamics, it is surprising that no *ab initio* calculations of their excited electronic states have been reported, with the exception of the lowest excited PES of ClCN.[28] The purpose of this paper is to provide such information for ClCN, since in this case spin–orbit interaction is small and can be neglected, thereby simplifying the calculations considerably. In view of the similarities between the electronic (and photoelectron) spectra of all the cyanogen halides,[32–34,36] we believe that many of the findings regarding ClCN and its electronic states are germane also to ICN and BrCN. Since for ICN it is believed that excitation in the A continuum involves singlet–triplet transitions, we carried out calculations on low-lying triplet states as well.

We find that even the case of ClCN poses problems in the *ab initio* calculations. These problems are caused by the proximity of Rydberg states to the low-lying singlet states, and the linear geometry of the molecule which leads to inconvenience in dealing with degenerate states. Nevertheless, we are able to show that the lowest excited states of the cyanogen halides derive from the $\pi^3\sigma^*$ configuration, but states deriving from the $\pi^3\pi^*$, and even the $\sigma\pi^4\sigma^*$, configurations are close by. This gives rise to a large manifold of excited states in the region of the A continuum, thereby increasing the probability of simultaneous excitation to more than one surface. Furthermore, we show that during the dissociation there are many opportunities for avoided crossings, conical intersections, and nonadiabatic transitions especially between the linear and bent triplet states. The implications of these findings to the photodissociation dynamics of ClCN and ICN are discussed.

II. COMPUTATIONAL DETAILS AND RESULTS

Most of the calculations reported here were carried out with the same Gaussian basis set as was previously used, the Dunning's[37] double zeta quality (9*s*5*p*/4*s*2*p*) contracted atomic orbital basis set augmented by a set of six d polarization functions on each atom with Gaussian exponents of 0.60 for chlorine, 0.75 for carbon, and 0.80 for nitrogen. Hartree–Fock calculations were performed using the GAUSSIAN 86 system of programs.[38] In order to overcome the shortcomings of the SCF calculations in describing virtual molecular orbitals, improved virtual orbitals (IVOs),[39] which are generated from the ground state wave functions and are the variational correct approximations to the self-consistent orbitals for the excited state, were implemented. This resulted in a significant improvement in the calculation of the PESs, and especially the dissociation energy.

Large scale configuration interaction (CI) calculations involving all single- and double-hole excitations from a multiconfiguration set of reference configurations were carried out. The $n = 1$ electrons of all three atoms were frozen. The reference configurations were chosen on the basis of their importance to the electronic state under study, and the resulting CI program was solved using the program PEPCI.[40] As a general rule, all configurations which had a coefficient in the final wave function greater than 0.1 were included in the reference space. All geometries were optimized by the finite difference method using the quadratic fitting function.

Two basis sets were used in the calculations. We found that the compact basis set used in our previous calculations of the low-lying electronic states of ClNO was usually adequate (basis a).[41] However, since the first Rydberg states of ClCN lie at $\sim$8.5 eV,[4,33,34] we supplemented the basis set with radially expanded (Rydberg) functions centered on C, N, and Cl (basis b), in order to obtain the Rydberg states. We find that the virtual orbitals have substantial (>0.3) Rydberg character, spread over all three atoms, and its inclusion results in lowering of the energies of some high-lying states by up to 0.3 eV. Thus, radially expanded orbitals having s and p Rydberg functions with exponents 0.044 for carbon, 0.064 for nitrogen, and 0.048 for chlorine were used in basis b.[42] For non-Rydberg states, the results with and without the Rydberg functions were quite similar (see below).

The experimental equilibrium geometry of ClCN is $r_{CN} = 1.163$ Å, $r_{CCl} = 1.629$ Å, and $\angle ClCN = 180°$,[43] and 15 molecular orbitals (MOs) are occupied in the ground state.[32] For linear geometry, the MOs principally involved in the excited states and obtained by using SCF (without IVO) with a basis set without Rydberg functions (basis a) are listed in Table I along with their energies. In order to limit the necessary CI size, it is computationally convenient to lower the molecular symmetry in order to split the degenerate shells. To remove these degeneracies in a systematic way, we lowered the molecular symmetry to C_s by slightly bending ClCN to 170°. The resulting molecular orbitals are listed in Table II, and the correspondence between the $C_{\infty v}$ and C_s orbitals is presented in Table III. In Table II we used SCF with IVO in the calculations of the molecular orbitals, and we give the orbital energies obtained with and without the Rydberg basis functions. The main cause for lowering of the energies of the virtual orbitals is the Rydberg basis functions, rather than the slight bending of the molecule or the inclusion of IVOs. The changes in energy upon bending are in the direction expected from the Walsh diagrams.[35,44] The slight

TABLE I. SCF molecular orbitals (without IVO) involved in the lowest excited states of ClCN; $\angle ClCN = 180°$, basis set a.

Symmetry	MO	Eigenvalue (a.u.)	Description[a]
$4\pi^*$	18	0.178 20	$Clp_x - CN\pi_x^*$
$4\pi^*$	17	0.178 20	$Clp_y - CN\pi_y^*$
$10\sigma^*$	16	0.172 78	$ClCN\sigma_z^*$
3π	15	−0.464 97	$Clp_y - CN\pi_y$
3π	14	−0.464 97	$Clp_x - CN\pi_x$
9σ	13	−0.598 45	$Clp_z - CN\sigma_z$
2π	12	−0.598 64	$Clp_y + CN\pi_y$
2π	11	−0.598 64	$Clp_x + CN\pi_x$

[a] The z axis is along the molecular internuclear axes.

TABLE II. SCF molecular orbitals (with IVO) involved in the excited states of ClCN;[a] ∠ClCN = 170°.

Symmetry	MO	Eigenvalue (a.u.) Basis set *a*	Eigenvalue (a.u.) Basis set *b*	Description
16 *a'**	20		0.130 62	Rydberg[b]
15 *a'**	19		0.111 46	Rydberg[b]
14 *a'**	18	0.204 77	0.111 41	$Clp_z + CN\sigma^*_{x,y}$ (+ Ryd)[b]
4 *a"**	17	0.177 82	0.085 31	$Clp_y - CN\pi^*_y$ (+ Ryd)[b]
13 *a'**	16	0.146 21	0.051 46	$Clp_{x,z} - CN\sigma^*_{x,z}$ (+ Ryd)[b]
12 *a'*	15	− 0.464 47	− 0.467 50	$Clp_x - CN\pi_x$
3 *a"*	14	− 0.464 96	− 0.467 99	$Clp_y - CN\pi_y$
11 *a'*	13	− 0.585 84	− 0.589 42	$Clp_z - CN\sigma_z$
2 *a"*	12	− 0.598 38	− 0.601 20	$Clp_y + CN\pi_y$
10 *a'*	11	− 0.598 46	− 0.601 28	$Clp_x + CN\pi_x$

[a] Basis set *a* is not augmented by Rydberg orbitals; basis set *b* incorporates *s* and *p* Rydberg functions on all three atoms in the IVOs (MOs 16–20).
[b] The Rydberg functions were used only in basis set *b*.

bending affects neither the energy of the electronic states nor their relative order in a significant way, and its main outcome is splitting the degenerate π orbitals lying in the y and x directions (the z direction is along the linear ClCN internuclear axis) into a' and a'' orbitals.

The highest occupied molecular orbitals are MO 14 and 15, which are degenerate at 180° (Table I), and are mainly π nonbonding, with a bonding configuration between C and N and an antibonding configuration between Cl and C. MO 13 is a nonbonding σ orbital lying along the molecular axis, and having its largest coefficient on the N atom. MOs 11 and 12 are a pair of degenerate bonding π orbitals where all the p orbitals are in-phase. In contrast with the electronic structure of ClNO, where the HOMOs (highest occupied) consist largely of nonbonding orbitals centered on Cl, in ClCN the MOs are delocalized with substantial coefficients on all atoms, and are thus true molecular orbitals. This, of course, is a consequence of the similar electronegativities of Cl and CN. In ICN, we expect less delocalization, as indeed confirmed by its photoelectron spectrum.[36] The LUMO (lowest unoccupied) is MO 16, which is σ antibonding, with the σ^* character delocalized along the two bonds. On the other hand, MOs 17 and 18, which are π antibonding, are mainly localized on the CN moiety, and promotion of an electron to these orbitals is expected to weaken the CN bond. For linear geometries, excitation from MOs 14 or 15 to MO 16 yields $^{1,3}\Pi$ states ($\pi^3\sigma^*$ configuration), whereas excitation to MOs 17 or 18 leads to $^{1,3}\Sigma^+$, $^{1,3}\Sigma^-$, and $^{1,3}\Delta$ states ($\pi^3\pi^*$ configuration), all in linear geometry.

TABLE III. Correlation of symmetry representations on molecular orbitals among the point groups of importance.

$C_{\infty v}$	C_s
$4\pi^*$	$15a'^*$ $14a''^*$
$10\sigma^*$	$3a'^*$
3π	$12a'$ $3a''$
9σ	$11a'$
2π	$2a''$ $10a'$

The order of the occupied orbitals and their nature are in agreement with the photoelectron spectroscopy results that field ClCN ionization potentials of 12.3, 13.8, and 15.3 eV assignable to ionization of electrons from π-nonbonding, σ_N-nonbonding, and π-bonding orbitals, respectively.[36] In addition, the vibrational structure in the photoelectron spectrum suggests significant delocalization of the occupied π orbitals, in agreement with the present calculations.[36]

The calculated vertical excitation energies are summarized in Table IV. The calculations were done with an initial geometry of 170°, and with basis sets excluding (basis *a*) and including (basis *b*) Rydberg functions. Clearly, the Rydberg functions have relatively small effect on the relative excitation energies and are important mainly for high-lying valence states and Rydberg states. We find that the angular dependences and the effects of stretching the Cl–C bond on the states' energies do not change significantly upon the addition of the radially expanded functions. Since the Rydberg functions are important only at high energies, and the calculations with basis set *b* are much more time consuming than with the more compact basis set *a*, the former was used only in calculations of the vertical excitation energies, whereas basis set *a*, which has proven to be quite successful before,[41,45] was used for calculations of angular dependences and minimum energy paths for the lower states. Since the calculations were performed at 170° geometry, the electronic states are listed in the their C_s symmetry notation. In cases where the angular dependence shows that the upper state is linear, the $C_{\infty v}$ notation is given in parentheses (see below).

The most intriguing feature in Table IV is that there are *three* electronic configurations that lead to close-lying valence states, $\pi^3\sigma^*$, $\pi^3\pi^*$, and $\sigma\pi^4\sigma^*$. For the low-lying triplet states, the energy difference between states arising from the

TABLE IV. Vertical excitation energies and oscillator strengths.

State	Primary excitation	Vertical energy (eV)[a] Basis *a*	Basis *b*	f_{calc} (basis *b*)	Optimized geometry[b] r_{CN}	∠ClCN
$1\,^1A'(1\,^1\Sigma^+)$[c]		0.00	0.00		1.16	180°
$1\,^3A'$	$16_{a'}(\sigma^*)\leftarrow 15_{a'}(\pi)$	6.17	6.19		1.17	117°
$1\,^3A''$	$16_{a'}(\sigma^*)\leftarrow 14_{a''}(\pi)$	6.58	6.61		1.17	130°
$2\,^3A'(1\,^3\Sigma^+)$[c]	$17_{a''}(\pi^*)\leftarrow 14_{a''}(\pi)$	6.92	6.92		1.32	180°
$1\,^1A''$	$16_{a'}(\sigma^*)\leftarrow 14_{a''}(\pi)$	7.40	7.26	1×10^{-2}	1.17	130°
$2\,^3A''(1\,^3\Delta)$[c]	$17_{a''}(\pi^*)\leftarrow 15_{a'}(\pi)$	7.50	7.48		1.32	180°
$2\,^1A'$	$16_{a'}(\sigma^*)\leftarrow 15_{a'}(\pi)$	7.88	7.66	2×10^{-2}	1.17	126°
$3\,^3A'(2\,^3\Delta)$[c]	$18_{a'}(\pi^*)\leftarrow 15_{a'}(\pi)$	7.86	7.77		1.32	180°
$2\,^1A''(1\,^1\Delta)$[c]	$17_{a''}(\pi^*)\leftarrow 15_{a''}(\pi)$	8.19	8.19	1×10^{-3}	1.32	180°
$3\,^3A''(1\,^3\Sigma^-)$[c]	$18_{a'}(\pi^*)\leftarrow 14_{a''}(\pi)$	8.24	8.22			
$4\,^3A'$	$16_{a'}(\sigma^*)\leftarrow 13_{a'}(\sigma)$	8.51	8.36		1.17	136°
$4\,^3A''$	$17_{a''}(\pi^*)\leftarrow 13_{a'}(\sigma)$	8.57	8.58			
$3\,^1A''$	$18_{a'}(\pi^*)\leftarrow 14_{a''}(\pi)$	8.91	8.74	2×10^{-3}		
$3\,^1A'(2\,^1\Delta)$[c]	$17_{a''}(\pi^*)\leftarrow 14_{a''}(\pi)$	8.94	8.79	3×10^{-3}	1.32	180°
	$18_{a'}(\pi^*)\leftarrow 15_{a'}(\pi)$					
$5\,^3A'$	$19_{a'}(\sigma^*)\leftarrow 15_{a'}(\pi)$		9.20			
$5\,^3A''$	$19_{a'}(\sigma^*)\leftarrow 14_{a''}(\pi)$		9.21			
$4\,^1A'$	$16_{a'}(\sigma^*)\leftarrow 13_{a'}(\sigma)$	9.61	9.38	4×10^{-2}	1.17	136°
$5\,^1A'$	$19_{a'}(\sigma^*)\leftarrow 15_{a'}(\pi)$		9.51	1×10^{-2}		
$4\,^1A''$	$19_{a'}(\sigma^*)\leftarrow 14_{a''}(\pi)$		9.54	1×10^{-4}		
$6\,^3A'$	$16_{a'}(\sigma^*)\leftarrow 11_{a'}(\pi)$		9.92			
$6\,^3A''$	$16_{a'}(\sigma^*)\leftarrow 12_{a''}(\pi)$		9.95			
$5\,^1A''$	$17_{a''}(\pi^*)\leftarrow 13_{a'}(\sigma)$		9.98	6×10^{-2}		
$7\,^3A'$	$18_{a'}(\pi^*)\leftarrow 13_{a'}(\sigma)$		10.20			
$7\,^3A''$	$20_{a'}(\sigma^*)\leftarrow 14_{a''}(\pi)$		10.64			
$6\,^1A''$	$16_{a'}(\sigma^*)\leftarrow 12_{a''}(\pi)$		10.67	6×10^{-2}		
$7\,^1A''$	$20_{a'}(\sigma^*)\leftarrow 14_{a''}(\pi)$		10.74	7×10^{-2}		
	$16_{a'}(\sigma^*)\leftarrow 12_{a''}(\pi)$					
$6\,^1A'$	$18_{a'}(\pi^*)\leftarrow 13_{a'}(\sigma)$		10.80	5×10^{-2}		
	$16_{a'}(\sigma^*)\leftarrow 11_{a'}(\pi)$					
$7\,^1A'$	$16_{a'}(\sigma^*)\leftarrow 11_{a'}(\pi)$					
	$18_{a'}(\sigma^*)\leftarrow 13_{a'}(\sigma)$		10.98	2×10^{-1}		

[a] In both cases, the calculations were performed at the experimental equilibrium geometry: $r_{CCl} = 1.629$ Å, $r_{NC} = 1.163$ Å, ∠ClCN = 170°. (Ref. 43).

[b] Geometry optimized at $r_{CCl} = 1.629$ Å.

[c] These states have linear configurations, but are given here in C_s symmetry notation, since the calculations were done at 170°.

first two configurations is less that 1 eV, and less than 2 eV between states arising from the $\pi^3\sigma^*$ and $\sigma\pi^4\sigma^*$ configurations. This is very different from the behavior of ClNO, where all the low-lying triplet states between 1.75 and 4.48 eV arise from a single electronic configuration.[41] The multiconfigurational excitations give rise to a large number of close-lying singlet and triplet states, thereby providing opportunities for adiabatic and nonadiabatic curve crossings.

The angular potential variations of some of the states are calculated in the Franck–Condon (FC) region, and the results are presented in Table V and Fig. 1. The linear or bent preferred geometries for these states are quite apparent. Geometry optimization near the FC region ($r_{ClC} = 1.629$ Å) of some of the low-lying states shows that the electronically excited states can be divided into two distinct groups; states arising from the $\pi^3\sigma^*$ and $\sigma\pi^4\sigma^*$ configurations are bent, with ∠ClCN = 117–140°, whereas triplet states deriving from the $\pi^3\pi^*$ configuration have their minimum energy at the linear geometry.

The dynamics of the photofragmentation of ClCN to $Cl(^2P_{1/2,3/2}) + CN(X\,^2\Sigma^+)$ depends on the nature of the PES along the dissociation coordinate. We therefore calculated least energy paths for several low-lying electronic states as a function of the Cl–C bond length. The results of the calculations for the bent states that correlate with $Cl(^2P_{1/2,3/2}) + CN(X\,^2\Sigma^+)$ are summarized in Table VI and Fig. 2. The calculations, which cover the range $r_{ClC} = 1.6$–3.0 Å, show that these bent states are purely repulsive. Although at $r_{ClC} = 3.0$ Å the state energies and r_{CN} have not quite reached their asymptotic values, we adopt this value as approximately representing full dissociation.

More intriguing is the behavior of states arising from the

TABLE V. Angular potential energy variation of some states of ClCN.

ClCN (deg)	Energy (eV)							
	$1\,^1A'(1\,^1\Sigma^+)$	$1\,^3A'$	$1\,^3A''$	$2\,^3A'(1\,^3\Sigma^+)$	$1\,^1A''$	$2\,^3A''(1\,^3\Delta)$	$2\,^1A'$	$4\,^3A'$
90°	3.57	6.20	6.89	10.12	7.81	9.35	7.43	8.92
100°	2.89	5.19	6.09	9.32	7.02	9.15	6.88	8.19
110°	2.12	4.65	5.65	8.64	6.46	8.70	6.59	7.50
120°	1.46	4.43	5.34	8.13	6.11	8.25	6.42	7.06
130°	0.96	4.49	5.25	7.83	6.00	8.13	6.40	6.80
140°	0.59	4.71	5.36	7.54	6.10	8.00	6.59	6.76
150°	0.31	5.07	5.62	7.33	6.42	7.82	6.88	7.02
160°	0.07	5.57	6.03	7.02	6.86	7.70	7.32	7.55
170°	0.03	6.20	6.60	6.98	7.37	7.66	7.82	8.17

[a] Energy relative to $1\,^1A'E_{eq} = -552.161\,111\,9$ a.u., at the calculated equilibrium bond distance: $r_{CCl} = 1.63$ Å, $r_{CN} = 1.16$ Å, ∠ClCN = 180°.

$\pi^3\pi^*$ configuration. These states derive from leading 18,17←14,15 excitations in the FC region. According to Table V and Fig. 1, the electronic states associated with this configuration are linear Σ and Δ states. Optimization of the CN bond length yields $r_{CN} = 1.32$ Å, and a linear geometry. The large change in r_{CN} from its ground state value reflects the localized nature of the π^* orbital on CN that weakens the bond, thereby causing its significant elongation.

The calculations of the minimum energy paths for states deriving from $\pi^3\pi^*$ excitation as a function of C–Cl bond length show evidence of avoided crossings between states of similar symmetry (C_s point group) deriving from the $\pi^3\pi^*$ and $\pi^3\sigma^*$ configurations. For example, following the minimum energy path of the lowest triplet state deriving from the $\pi^3\pi^*$ configuration, the $2\,^3A'(17_{a''} \leftarrow 14_{a''})$ state, we find a barrier near $r_{CCl} = 1.9$ Å whose height is ~0.2 eV above the minimum energy at $r_{CCl} = 1.6$ Å (see Table VII). At $r_{CCl} < 1.9$ Å, the principal excitation in $2\,^3A'$ is 17←14, the geometry is linear and the optimized r_{CN} is 1.32 Å. At $1.9 \leqslant r_{CCl} < 2.2$ Å, the leading excitations are 16←13 and

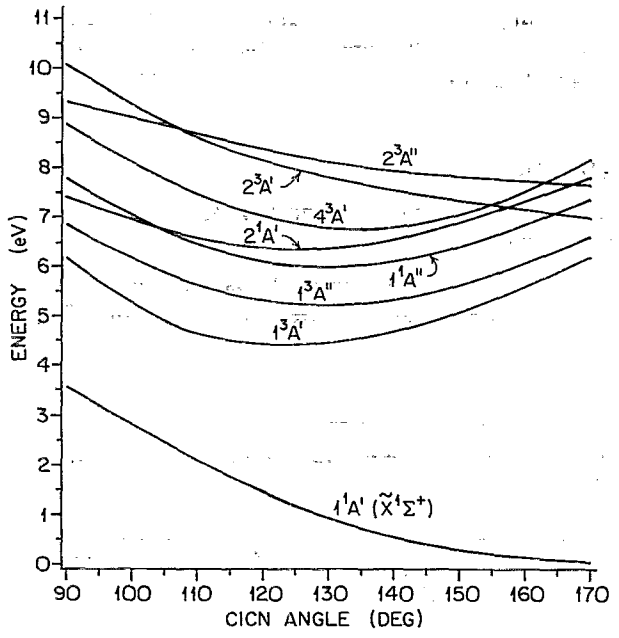

FIG. 1. The angular dependence of the potential surfaces at the Franck–Condon region; $r_{CCl} = 1.629$ Å; $r_{CN} = 1.17$ Å.

TABLE VI. Geometrically optimized potential energy surfaces of ClCN for some electronic states which lead to $CN(X\,^2\Sigma^+) + Cl(^2P)$.

State	r_{CCl} (Å)	r_{CN} (Å)	ClCN(deg)	Energy(eV)[a]
$1\,^1A'$	1.63	1.160	180°	0.00
	1.80	1.180	180°	0.36
	2.00	1.185	180°	1.38
	2.20	1.190	180°	2.41
	2.60	1.190	180°	3.55
	3.00	1.190	180°	4.17
$1\,^3A'$	1.60	1.170	130°	4.66
	1.80	1.170	135°	4.55
	2.00	1.180	135°	4.51
	2.20	1.180	135°	4.47
	2.60	1.185	140°	4.44
	3.00	1.190	140°	4.43
$1\,^3A''$	1.60	1.170	130°	5.48
	1.80	1.170	130°	5.01
	2.00	1.175	130°	4.80
	2.20	1.185	135°	4.64
	2.60	1.185	135°	4.53
	3.00	1.190	140°	4.48
$1\,^1A''$	1.60	1.170	130°	6.26
	1.80	1.170	130°	5.58
	2.00	1.180	130°	5.36
	2.20	1.180	130°	5.16
	2.60	1.185	140°	4.84
	3.00	1.190	140°	4.70
$2\,^1A'$	1.60	1.170	125°	6.66
	1.80	1.170	125°	5.99
	2.00	1.180	125°	5.55
	2.20	1.185	135°	5.27
	2.60	1.185	140°	4.94
	3.00	1.190	140°	4.62

[a] Energies relative to $1\,^1A'E_{eq} = -552.161\,111\,9$ a.u. at the calculated equilibrium geometry: $r_{CCl} = 1.63$ Å, $r_{CN} = 1.16$ Å, ∠ClCN = 180°.

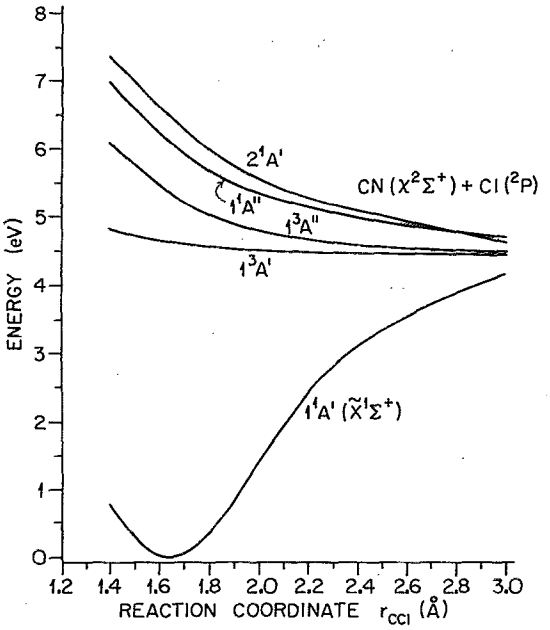

FIG. 2. Optimized least energy paths along the reaction coordinate, r_{CCl}, for electronic states correlating with $Cl(^2P) + CN(X^2\Sigma^+)$ products. In the calculations, r_{CN} and ∠ClCN were optimized as a function of r_{CCl}.

16←11, and the state is bent with optimized ∠ClCN = 140° and r_{CN} = 1.22 Å. Although the barrier is small and almost within the error of the calculations (± 0.1 eV), the change in the leading orbital excitations suggests an avoided crossing.

When we follow the lowest state with leading 17←14 excitation, we observe a different behavior. Up to r_{CCl} = 1.8 Å, this is the leading excitation in the $2\,^3A'$ state (see Table VIII), as described above. However, at $r_{CCl} > 1.8$ Å, we find that the 17←14 excitation appears as an important configuration in several excited states which are higher in energy than the $2\,^3A'$ state. Each of these state is described by several excited configurations. The optimized energies of the lowest of these states are given in Table VIII as a function of r_{CCl}. A fast increase in energy with increasing r_{CCl} is obtained for $r_{CCl} > 1.9$ Å, and orbital excitations 16←13 and 18←15 contribute significantly to the state, in addition to the 17←14 excitation. Thus, around r_{CCl} = 1.9 Å, there is evidence for surface crossing affecting the $2\,^3A'$ state. The natural candidates for participation in this avoided crossing are the $4\,^3A'$ and $6\,^3A'$ states, whose leading excitations in the FC region are 16←13 and 16←11, respectively (see Table IV). It is quite likely that multiple avoided crossings affect some of the other upper states, leading to the mixed configurations observed at large r_{CCl}.

Another cut in the potential that has implications to the dissociation dynamics is given in Table IX. Here, r_{CN} in the $2\,^3A'$ state is fixed at its FC value, 1.17 Å, and only the bond angle is optimized. We find that at r_{CCl} = 1.6–2.2 Å, the optimized ClCN angle is 130°, and the energy decreases monotonically with increasing r_{CCl}. However, upon bending, the leading excitation changes to a combination of 16←13 and 16←11. This shows that near the FC region, there are strong bending forces affecting at least some linear excited states of $\pi^3\pi^*$ configuration.

Our calculations show that six states ($3\times A'$ and $3\times A''$ in C_s symmetry) correlate with ground state products and, in addition, we identify four states, $^{1,3}A'$ and $^{1,3}A''$, that correlate with $Cl(^2P) + CN(A\,^2\Pi)$. The states deriving from the $\pi^3\pi^*$ configuration correlate apparently with highly excited states of free CN, and possible candidates are the $E\,^2\Sigma^+$ and $F\,^2\Delta$ states (r_{CN} = 1.3245 and 1.3732 Å, respectively).[46]

TABLE VII. Minimum energy path for the $2\,^3A'$ state of ClCN.[a]

r_{CCl} (Å)	r_{CN} (Å)	∠ClCN (deg)	E (eV)
1.5	1.32	170°	6.20
1.6	1.32	170°	5.76
1.7	1.32	170°	5.84
1.8	1.30	170°	5.89
1.9	1.22	140°	5.97
2.0	1.22	140°	5.61
2.2	1.21	135°	5.27

[a] Calculated with basis set *a* and equilibrium bending angle 170°. Energies relative to $1\,^1A'E_{eq} = -552.161\,1$ a.u. at the calculated equilibrium geometry.

TABLE VIII. Optimized geometries for the lowest triplet state with dominant 17←14 ($\pi^3\pi^*$) excitation.[a]

r_{CCl} (Å)	r_{CN} (Å)	∠ClCN (deg)	E (eV)
1.5	1.32	170°	6.20
1.63	1.32	170°	5.78
1.8	1.30	170°	5.89
1.9	1.30	170°	6.04
2.0	1.30	170°	6.34
2.2	1.32	170°	7.33

[a] See footnote to Table VII.

III. DISCUSSION

A. Electronic spectroscopy and comparisons with experimental results

Several experimental observations can be compared with the calculated results; the electronic spectrum, Cl–CN

TABLE IX. Optimized ∠ClCN for the $2\,^3A'$ state, with r_{CN} = 1.17 Å.[a]

r_{CCl} (Å)	r_{CN} (Å)	∠ClCN (deg)	E (eV)
1.63	1.17	130°	6.84
1.8	1.17	130°	6.36
1.9	1.17	130°	6.00
2.0	1.17	130°	5.66
2.2	1.17	130°	5.33

[a] See footnote to Table VII.

bond dissociation energy, photoelectron spectrum and photodissociation dynamics. The photoelectron spectrum is compared with the theoretical results in Sec. II and shows good qualitative agreement with the calculations. We find, in agreement with experiment, that the highest occupied MOs consist of two pairs of delocalized nonbonding and bonding π orbitals, and a σ_N nonbonding orbital whose energy is between the two pairs of π orbitals. More intriguing is the proximity of the calculated π^* and σ^* virtual orbitals, leading to the appearance of close-lying excited states of both $\pi^3\pi^*$ and $\pi^3\sigma^*$ configurations.

The ClCN bond dissociation energy $[\mathrm{ClCN} \rightarrow \mathrm{Cl}(^2P) + \mathrm{CN}(X\,^2\Sigma^+)]$ can be estimated from the asymptotic energies at $r_{CCl} = 3.0$ Å. We find that the energy of the ground state is 4.17 eV above the value at the equilibrium geometry, and still rising slowly with r_{CCl}. The average energy of the four repulsive bent states that correlate with ground state products at the same r_{CCl} separation is 4.56 eV, and still slowly going down. The average of all the repulsive states correlating with ground state products and corrected for zero-point energies is 4.4 eV, in good agreement with the experimental value of 4.33 eV.[47] In these calculations, IVOs and basis set *a* were employed.

The interpretation of the electronic spectra of the cyanogen halides has been the subject of continued debate, as discussed in Sec. I. There is no clear theoretical preference for choosing between the $\pi^3\pi^*$ and $\pi^3\sigma^*$ as the electronic configuration responsible for the first singlet excited state. Our results show unambiguously that the lowest two singlet excited states in ClCN are a pair of $^1A'$ and $^1A''$ states (C_s point group) deriving from the $\pi^3\sigma^*$ electronic configuration, and correlating with a $^1\Pi$ linear state. The vertical energies of these states, 7.26 and 7.48 eV above the ground state, are close to the location of the peak in the lowest, structureless absorption feature known the *A* continuum, which is at ~7.0 eV.[33,34] The absorption band extends from ~170 nm (7.3 eV) to ~210 nm (5.9 eV). The calculated oscillator strengths for the $2\,^1A''$ and $1\,^1A'$ states are 1.7×10^{-2} and 5.9×10^{-2}, respectively. These are upper limits and the observed values are expected to be reduced by the unfavorable FC factors for the linear–bent transitions. Thus, the calculations are in satisfactory agreement with the measured oscillator strength of the *A* continuum (4.8×10^{-3} and 6.5×10^{-3}).[33,34] We therefore assign the *A* continuum to excitations to the bent $2\,^1A'$ and $1\,^1A''$ states, with the latter probably contributing more to the long-wavelength side of the absorption band. The bent nature of the states is in agreement with the observation of highly excited, inverted $\mathrm{CN}(X\,^2\Sigma^+)$ rotational distributions obtained upon 190–213 nm photolysis, which are typical of dissociation with a large torque.[23] Preliminary, unanalyzed rotational-alignment results show some polarization in the $\mathrm{CN}(B\,^2\Sigma^+ \leftarrow X\,^2\Sigma^+)$ laser induced fluorescence signal; however, the results are dependent on photolysis wavelength, indicating the participation of more than one PES in this wavelength region.[23] More accurate results are needed for detailed comparisons with the calculations.

The analysis of the next higher absorption features at 8.0–10.0 eV is less straightforward, but the spectrum likely consists of both valence and Rydberg transitions.[4,33,34] The latter are assigned to the relatively sharp features known as the *B* and *C* bands.[33] Macpherson and Simons assign the transitions originating at 73 965 cm^{-1} (9.17 eV) and 74 460 cm^{-1} (9.23 eV) to the $^{1,3}\Pi$ Rydberg transitions,[48] whereas Felps *et al.* assign the origin of these transitions at 70 075 cm^{-1} (8.7 eV) and 71 380 cm^{-1} (8.85 eV).[34] The first calculated triplet and singlet Rydberg states have their vertical excitation energies at 9.2 and 9.4 eV, respectively, in fair agreement with the experimental assignments of the *B* and *C* bands, whose strongest bands appear around 9.2 eV.[33] Felps *et al.* find, in addition, a broad underlying absorption feature, which they attribute to valence excitation to a state deriving from the $\pi^3\pi^*$ configuration. Its origin is tentatively assigned at 62 050 cm^{-1} (7.7 eV) and its maximum is at 68 650 cm^{-1} (8.5 eV).[34] In our calculations we find two relatively strong transitions with $\pi^3\pi^*$ excited state configurations, whose vertical transition energies are ~8.7 eV (see Table IV), in good agreement with the assignment of Felps *et al.* The experimental data show that the absorption band is broad and exhibits an oscillatory structure with somewhat irregular intervals of 600–700 cm^{-1}. The oscillations may have a similar explanation as in the $B\,^1A_1 \leftarrow X\,^1A_1$ spectrum of water, and may represent resonances or periodic orbits,[49] although the similarity between the spectral spacings in the ClCN band and the C–Cl stretching frequency (744 cm^{-1} in the ground electronic state) has been noted.[34] Guest *et al.* determined the alignment parameter from the CN $B\,^2\Sigma^+ \leftarrow X\,^2\Sigma^+$ emission following photolysis at 157.6 nm in the same band system, and deduced that the transition is predominantly parallel.[29] A tentative assignment would then be the $3\,^1A'$ state. We find that the strongest absorptions occur at 10.67–10.98 eV, whereas experimentally the strongest absorption feature appears around 10 eV,[34] but the accuracy of the calculations at these high energies is not very good. The high density of electronic states between 8.7 and 11 eV makes simultaneous absorption to more than one surface quite probable and opportunities for surface crossings are abundant. Indeed, Simons and co-workers, who measured the polarization of the $\mathrm{CN}(B\,^2\Sigma^+)$ emission following 120–140 nm photolysis, found that the quantum yields for production of $\mathrm{CN}(B\,^2\Sigma^+)$ were low (<0.1), and did not exhibit the sharp bands which dominate the absorption spectrum in this region, but rather appeared like the underlying continuum.[4] Polarized emission was observed at many wavelengths, but no correlation with specific states was made.

We conclude that the lowest excited singlet and triplet states of ClCN arise from the $\pi^3\sigma^*$ configuration yielding bent $^{1,3}A'$ and $^{1,3}A''$ states. This is in agreement with the original assignment of King and Richardson and also with Felps *et al*[33,34] The theoretical calculations of Waite and Dunlap also show that the first excited singlet state of ClCN is bent, but they assign it to $\pi^3\pi^*$ excitation.[28] The next higher valence singlet states in our calculations arise from the $\pi^3\pi^*$ configuration and the triplet states are all linear. The assignment of these states as Σ and Δ states is tentative and based mainly on the convergence of the two triplet states assigned as Δ ($C_{\infty v}$ point group) to a similar energy value

when the ClCN angle approaches 180°. The slight bending of ClCN used in our calculations affects neither the order nor the assignment of the excited states, and only very little their vertical energies.

B. Implications to the photodissociation dynamics of the cyanogen halides

$CN(X\,^2\Sigma^+)$ rotational distributions were measured following photodissociation of ClCN at several wavelengths within the A continuum.[23] The highly excited, inverted rotational distributions are nicely modeled both by quantal[27(b)] and classical[23,27(a),27(b)] calculations on a repulsive PES with bent equilibrium geometry.[28] However, at the long wavelength tail of the A continuum ($\geqslant$208 nm), the distributions change abruptly; they are still inverted, but peak at lower N'', and it is suggested that a second surface is responsible for these colder distributions. There is little doubt that the A continuum consists of excitations to the $2\,^1A'$ and $1\,^1A''$ states, and it is tempting to assign them as the surfaces responsible for the observed ClCN dissociation at 193–210 nm.[23] However, no photodissociation results at wavelengths <193 nm are available, nor are accurate recoil anisotropy and rotational alignment data that can aid in the correct assignment of the observed dissociative states. Also, one cannot rule out the possibility that the weak absorption tail ($\sigma < 3\times10^{-20}$ cm^{-1})[23] yielding the colder CN rotational distribution at photolysis wavelengths >208 nm arises from a forbidden singlet–triplet transition. The $1\,^3A'$ and $1\,^3A''$ states both have vertical energies near 200 nm (see Table IV), and we have found before that the spin–orbit interaction in Cl is sufficiently strong to induce singlet–triplet transitions by intensity borrowing from strong allowed transitions (e.g., in ClNO).[41] The experimental findings suggest that the surfaces responsible for dissociation of ClCN in the A continuum are all repulsive with bent equilibrium geometry, and we ascribe them to states deriving from the $\pi^3\sigma^*$ configuration.

A more intriguing and complex situation occurs upon dissociation on the triplet $2\,^3A'$ state, which involves avoided crossing(s) between one or more surfaces at $r_{CCl}\cong1.9$ Å. It appears that as the C–Cl bond length increases, triplet states with leading excitations arising from the $\pi^3\sigma^*$ and $\sigma\pi^4\sigma^*$ configurations (e.g., leading excitations $16\leftarrow13,12,11$) go down in energy, while the linear triplet states deriving from the $\pi^3\pi^*$ configuration go up in energy. Since there are several close-lying states in the 8–10 eV region, there are many opportunities for surface crossings and some were identified in our calculations (Sec. II). We note that in these calculations the linear states were slightly bent (170°), resulting in avoided crossings between states of the same symmetry (i.e., A' or A''). In reality, zero point bending motions or excitation of hot bands may provide the slight bending required to lower the symmetry from $C_{\infty v}$ to C_s, thereby encouraging surface crossings.[17] As can be seen from Table IX, there are strong bending forces acting in the FC region, and the optimum angle obtained when r_{CN} is fixed at its FC value (1.17 Å) is 130°. There are two forces acting on molecules dissociating on the $2\,^3A'$ ($\pi^3\pi^*$) surface; one tends to extend the CN bond to its optimum value, 1.32 Å, while the other acts to bend the ClCN angle (Table VII). The final CN energy distribution will therefore be very sensitive to the shape of the PES near the FC region, and to the bending motions that govern the couplings and avoided crossings along the reaction coordinate.

Although, strictly speaking, our results are germane only to ClCN, owing to the similarities among the electronic spectra of the cyanogen halides, they may also provide insights into the photodissociation dynamics of ICN in the A continuum (which is thought to involve singlet–triplet transitions).[4,20] In ICN spin–orbit interaction is particularly large (the iodine atom spin–orbit states are separated by 7603 cm^{-1}), and for linear–linear transitions, $\Delta\Omega = 0, \pm1$ transitions are allowed. The most detailed studies in the A continuum were done at 248 and 266 nm.[5–20] The measured scalar properties include the global $CN(X\,^2\Sigma^+)$ rotational distributions, and the individual rotational distributions correlating with $I(^2P_{3/2})$ and $I(^2P_{1/2})$ [reactions (1) and (2), respectively]. Vector properties include measurements of the anisotropy parameter β, the rotational alignment parameter, $A_0^{(2)}$, and the orientation parameter $A_0^{(1)}$.

The $CN(X\,^2\Sigma^+)$ rotational distributions obtained following dissociation of ICN at 235–280 nm are all multimodal; they have at least one distinct component peaking at low N″, and one component peaking at high N″.[8] Pitts and Baronavsky,[21] and later Hess and Leone[22] showed that at these wavelengths, both $I(^2P_{3/2})$ and $I(^2P_{1/2})$ are produced [channels (1) and (2), respectively]. Nadler *et al.*, using sub-Doppler resolution spectroscopy to dissect the CN rotational distributions into two separate contributions from channels (1) and (2), found that at 266 nm low and high N″ are associated predominantly with $I(^2P_{1/2})$ [reaction (2)] and $I(^2P_{3/2})$ [reaction (1)], respectively.[9] It was proposed that reactions (2) and (1) are associated with linear and bent surfaces, respectively.[9] The recoil anisotropy parameters for the two channels were unequal [$\beta(I^2P_{1/2}) = 1.6 \pm 0.2$; $\beta(I^2P_{3/2}) = 1.3 \pm 0.2$], but within each channel β did not vary significantly with N″. Using a similar technique, Black *et al.* showed recently that at 248 nm, the β parameters are N″ dependent; N″ levels correlated with channel (2) yielded $\beta = 1.85$, and the CN rotational distribution was cold, while those correlated with channel (1) showed two distinct regions, $\beta = \sim -0.5$ for N″ = 0–25, while for higher N″, β increased monotonically with N″ up to a value of ~1.0.[6]

The experimental observations are straightforward, and measurements of different vector properties lead to the same conclusions regarding the polarizations of the transitions involved and their dependence on N″.[5–12] The interpretation of these data, however, is not unambiguous. With 266 nm photolysis, the initial absorption was assumed to involve a parallel transition to a linear surface correlating with channel (2), which is then coupled to the surface responsible for channel (1).[9] This interpretation reconciled all the experimental observations at 266 nm, except the decrease in the value of β following surface crossing, for which only tentative explanations have been offered. Black *et al.* interpreted their results at 248 nm in terms of at least three surfaces: two

bent surfaces correlating with channel (1) [one associated with a perpendicular transition (low–medium N″), and the other with a parallel transition (medium–high N″)], and a linear surface, reached via a parallel transition, correlating with channel (2).[6] They proposed that the linear surface and the bent surface with $\beta \sim -0.5$ are accessed directly, while the bent surface with positive β is reached via surface crossings with the linear surface.[6]

If we assume that, except for a much stronger spin–orbit interaction, the excited state configurations in ICN are similar to those of ClCN, we may start to appreciate the complexity of the photodissociation dynamics of ICN. For example, our calculations indicate that excitation via the $0^+ \leftarrow 0^+$ linear–linear transition (e.g., to the triplet states deriving from the $\pi^3\pi^*$ configuration) would give rise to a parallel transition. In the limit of linear molecule and Hund's case (c), as is proper for ICN, $^3\Pi$ states will split into $0^+, 0^-$, 1 and 2 states, $^3\Sigma^-$ states will yield 1 and 0^+ distinct electronic surfaces, and Δ states—3,2, and 1 states. For bent excited states, there will be further splittings of each state with $\Omega > 0$ into A' and A'' states.[35] The opportunities then of coupling to other surfaces deriving from both the $\pi^3\pi^*$ and $\pi^3\sigma^*$ configurations are numerous, and several states can participate in avoided crossings, and nonadiabatic transitions during the dissociation.[51]

Also, recall that the coupling coefficients depend both on the energy and the molecular geometry, and thus may vary during the dissociation, thereby inducing crossings and recrossings during bond separation. For example, we find that at $1.9\ \text{Å} < r_{CCl} < 2.2\ \text{Å}$, many states become close in energy, enhancing the probability of curve crossings. In addition, the linear–bent geometry of many of the transitions can give rise to simultaneous excitations of A' and A'' surfaces that are Renner–Teller pairs (i.e., those states correlating with Π or Δ states in $C_{\infty v}$ symmetry), and are therefore degenerate in the linear configuration of the FC region.[52] In addition to direct excitation of states deriving from the $\pi^3\pi^*$ configuration, simultaneous optical excitation to one or more of the bent states deriving from the $^3\Pi$ state ($\pi^3\sigma^*$ configurations) cannot be ruled out, and transitions to A' and A'' states will give rise to additional parallel and perpendicular transitions. The relative importance of the different processes is likely to be a function of wavelength within the A continuum.

In view of this complexity, it is doubtful that with our present knowledge and theoretical capabilities a unique interpretation of the ICN results in the A continuum is forthcoming, and this complexity has been indeed highlighted in the most recent experimental studies.[6,7] In addition, two theoretical treatments achieved reasonable agreement with the experimental results assuming very different dissociation schemes; Marinelli *et al.* assumed direct excitation to three surfaces only minor effects due to nonadiabatic interactions,[8(a)] while Goldfield *et al.* succeeded to no lesser extent by building a model potential in which the initial excitation involved only one state, followed by nonadiabatic surface crossings.[14]

Following the fs experiments of Zewail and coworkers,[13] renewed interest in ICN as a model for dissociation on two coupled surfaces has emerged, and resulted in several recent theoretical publications.[15,18,19] Our calculations suggest that the assumption that only two surfaces are involved in the dissociation in the A continuum is likely to be an over simplication. Based on the experimental data, the *ab initio* calculations for ClCN, and the present discussion, we believe that it is unjustified to assume that a single electronic transition is responsible for the entire absorption spectrum in the A continuum, and that the model potentials used to date may be too simplified to describe the complex processes which occur during ICN dissociation.

IV. SUMMARY

(1) The low-lying excited states of ClCN derive from *three* electronic configurations leading to many close-lying singlet and triplet excited states. The lowest excited state derives from the $\pi^3\sigma^*$ configuration, but states deriving from the $\pi^3\pi^*$ and $\sigma\pi^4\sigma^*$ configurations are < 2 eV above the lowest excited state. This gives rise to a dense manifold of close-lying dissociative states, many of which can be accessed optically. The calculated vertical excitation energies are in good agreement with features in the absorption spectra of ClCN.

(2) The low-lying excited electronic states arising from the $\pi^3\sigma^*$ and $\sigma\pi^4\sigma^*$ configurations are bent, with equilibrium angles 117°–140°. The lowest states arising from the $\pi^3\pi^*$ configuration are linear.

(3) There is evidence of avoided crossings between states arising from the $\pi^3\pi^*$ configuration and those arising from the $\pi^3\sigma^*$ and $\sigma\pi^4\sigma^*$ configurations. The avoided crossings can be induced by slight bending of ClCN causing lowering of the symmetry from $C_{\infty v}$ to C_s.

(4) The A continuum of ClCN involves transitions to the bent $2^1A'$ and $1^1A''$ surfaces, with a possible excitation of the bent $1\ ^3A''$ surface at the weak, long-wavelength tail of the absorption band. This is in agreement with the experimental results on the photodissociation of ClCN, which yield highly rotationally excited $CN(X\ ^2\Sigma^+)$ and also suggests the participation of more than one surface across the A continuum.

(5) Based on the similarities between the electronic spectra of the cyanogen halides, and taking into account the large spin–orbit splitting in iodine, we believe that the A continuum in ICN consists of transitions to several surfaces whose contributions vary across the absorption band in agreement with recent experimental results.[6,8,21,22] Simultaneous excitations to more than one surface at each wavelength are possible,[6,8] and there are numerous opportunities for avoided crossings and nonadiabatic surface crossings during the dissociation.[6–12,14] These may involve more than two surfaces, as the couplings change along the reaction coordinate during the dissociation.

ACKNOWLEDGMENTS

We wish to thank C. X. W. Qian for helpful discussions, and J. B. Halpern for making results available to us prior to publication. One of us (H. R.) has benefited greatly from discussions with Robert W. Field on the spectroscopy of the

cyanogen halides and possible couplings between their electronic states. This research was supported by the National Science Foundation and the Army Research Office under the auspices of the Center for the Study of Fast Transient Processes.

[1] For a recent review see, W. M. Jackson and H. Okabe, Adv. Photochem. **13**, 1 (1985).
[2] (a) K. E. Holdy, L. C. Klotz, and K. R. Wilson, J. Chem. Phys. **52**, 4588 (1970); (b) J. H. Ling and K. R. Wilson, *ibid.* **63**, 101 (1975).
[3] G. A. Chamberlain and J. P. Simons, Chem. Soc. Faraday 2 **71**, 2043 (1975).
[4] M. N. R. Ashfold, M. T. MacPherson, and J. P. Simons, in *Topics in Current Chemistry* (Springer, Berlin, 1979), Vol. 36.
[5] Earlier work on ICN is referenced, in I. Benjamin and K. R. Wilson, J. Chem. Phys. **90**, 4176 (1989).
[6] J. F. Black, J. R. Waldeck, and R. N. Zare, J. Chem. Phys. **92**, 3519 (1990), and references cited therein.
[7] J. F. Black, E. Hasselbrink, J. R. Waldeck, and R. N. Zare, Mol. Phys. (in press).
[8] (a) W. J. Marinelli, N. Sivakumar, and P. L. Houston, J. Phys. Chem. **88**, 6685 (1984); (b) G. E. Hall, N. Sivakumar, and P. L. Houston, J. Chem. Phys. **84**, 2120 (1986).
[9] I. Nadler, D. Mahgerefteh, H. Reisler, and C. Wittig, J. Chem. Phys. **82**, 3885 (1985).
[10] (a) H. Joswig, M. A. O'Halloran, R. N. Zare, and M. S. Child, Faraday, Discuss. Chem. Soc. **82**, 79 (1986); (b) M. A. O'Halloran, H. Joswig, and R. N. Zare, J. Chem. Phys. **87**, 303 (1987).
[11] E. Hasselbrink, J. R. Waldeck, and R. N. Zare, Chem. Phys. **126**, 191 (1988).
[12] J. F. Black, J. R. Waldeck, E. Hasselbrink, and R. N. Zare, J. Chem. Phys. Soc. Faraday Trans. 2 **85**, 1044 (1989).
[13] (a) M. Dantus, M. J. Rosker, and A. H. Zewail, J. Chem. Phys. **87**, 2395 (1987); (b) **89**, 6128 (1988); (c) M. J. Rosker, M. Dantus, and A. H. Zewail, *ibid.* **89**, 6113 (1988); (d) A. H. Zewail, J. Chem. Soc. Faraday Trans. 2 **85**, 1221 (1989).
[14] E. M. Goldfield, P. L. Houston, and G. S. Ezra, J. Chem. Phys. **84**, 3120 (1986).
[15] H. Guo and G. C. Schatz, J. Chem. Phys. **92**, 1634 (1990).
[16] C. H. Dugan and D. Anthony, J. Phys. Chem. **91**, 3929 (1987).
[17] J. Vigué, B. Girard, G. Gouédard, and N. Billy, Phys. Rev. Lett. **62**, 1358 (1989).
[18] R. Heather and H. Metiu, Chem. Phys. Lett. **157**, 505 (1989).
[19] N. E. Henriksen and E. J. Heller, J. Chem. Phys. **91**, 4700 (1989).
[20] M. D. Morse, K. F. Freed, and Y. B. Band, J. Chem. Phys. **70**, 3620 (1979).
[21] W. M. Pitts and A. P. Baronavski, Chem. Phys. Lett. **71**, 395 (1980).
[22] W. P. Hess and S. R. Leone, J. Chem. Phys. **86**, 3773 (1987).
[23] S. A. Barts and J. B. Halpern, J. Phys. Chem. **93**, 7346 (1989).
[24] J. B. Halpern and W. M. Jackson, J. Phys. Chem. **86**, 3528 (1982).
[25] R. Lu, V. McCrary, J. B. Halpern, and W. M. Jackson, J. Phys. Chem. **88**, 3419 (1984).
[26] J. A. Russel, I. A. McLaren, W. M. Jackson, and J. B. Halpern, J. Phys. Chem. **91**, 3248 (1987).
[27] (a) R. Schinke and V. Engel, Faraday, Discuss. Chem. Soc. **82**, 111 (1986); (b) R. Schinke, Comments Atom. Mol. Phys. **23**, 15 (1989); (c) R. Schinke, J. Chem. Phys. **92**, 2397 (1990).
[28] B. A. Waite and B. I. Dunlap, J. Chem. Phys. **84**, 1391 (1986).
[29] J. A. Guest, M. A. O'Halloran, and R. N. Zare, Chem. Phys. Lett. **103**, 261 (1984).
[30] G. E. Hall and P. L. Houston, Annu. Rev. Phys. Chem. **40**, 375 (1989).
[31] See, for example, *Molecule Photodissociation Dynamics*, edited by M. N. R. Ashfold and J. E. Baggot (Royal Society of Chemistry, London, 1987).
[32] J. W. Rabalais, J. M. McDonald, V. Scherr, and S. P. McGlynn, Chem. Rev. **71**, 73 (1971).
[33] G. W. King and A. W. Richardson, J. Mol. Spectrosc. **21**, 339 353 (1966).
[34] W. S. Felps, S. P. McGlynn, and G. L. Findley, J. Mol. Spectrosc. **86**, 71 (1981).
[35] G. Herzberg, *Spectra of Diatomic Molecules* (Van Nostrand Reinhold, New York, 1950); (b) *Spectra of Polyatmoic Molecules* (Van Nostrand Reinhold, New York, 1966).
[36] R. F. Lake and H. Thompson, Proc. R. Soc. London, Ser. A **317**, 187 (1970).
[37] T. H. Dunning, Jr., J. Chem. Phys. **53**, 2823 (1970).
[38] J. S. Binkley, R. A. Whiteside, R. Krishnan, R. Seegar, D. J. Defrees, H. B. Schlegel, S. Topiol, L. R. Kahn, and J. A. Pople, Gaussian, Inc., Carnegie Mellon University, Pittsburgh, 1982.
[39] W. J. Hunt and W. A. Goddard III, Chem. Phys. Lett. **3**, 414 (1969).
[40] J. J. Diamond, G. A. Segal, and R. W. Wetmore, J. Phys. Chem. **88**, 3532 (1984).
[41] Y. Y. Bai, A. Ogai, C. X. W. Qian, L. Iwata, G. A. Segal, and H. Reisler, J. Chem. Phys. **90**, 3903 (1989).
[42] W. J. Hehre, L. Radom, P. R. Schleyer, and J. A. Pople, *Ab Initio Molecular Orbital Theory* (Wiley, New York, 1986).
[43] C. H. Townes, A. N. Holden, and F. R. Merriti, Phys. Rev. **74**, 1113 (1948).
[44] A. D. Walsh, J. Chem. Soc., 2266 (1953).
[45] (a) V. Marudarajan and G. A. Segal, Chem. Phys. Lett. **128**, 1 (1986); (b) S. Nagamani and G. A. Segal, J. Am. Chem. Soc. **108**, 6880 (1986).
[46] K. P. Huber and G. Herzberg, *Molecular Spectra and Molecular Structure. IV. Constants of Diatomic Molecules* (Van Nostrand Reinhold, New York, 1979).
[47] H. Okabe, *Photochemistry of Small Molecules* (Wiley, New York, 1978).
[48] M. T. MacPherson and J. P. Simons, J. Chem. Soc. Faraday Trans. 2 **75**, 1572 (1979).
[49] (a) E. Segev and M. Shapiro, J. Chem. Phys. **73**, 2001 (1970); (b) **77**, 5604 (1982).
[50] (a) K. Weide and R. Schinke, J. Chem. Phys. (i) **87**, 4627 (1987), (ii) *ibid.*; (b) K. Weide, J. Kühl, and R. Schinke, *ibid.* **91**, 3999 (1989).
[51] H. Lefebre-Brion and R. W. Field, *Perturbations in the Spectra of Diatomic Molecules* (Academic, Orlando, 1986).
[52] S. Carter, I. M. Mills, and R. N. Dixon, J. Mol. Spectrosc. **106**, 411 (1984).